Biophysical Journal, Volume *111*

Supplemental Information

Clathrin Assembly Regulated by Adaptor Proteins in Coarse-Grained Models

Matteo Giani, Wouter K. den Otter, and Wim J. Briels

Supplementary Material

Clathrin assembly regulated by adaptor proteins in coarse-grained models

M. Giani, [1,2,3] W.K. den Otter [1,2,3] and W.J. Briels [2,3,4]

[1] Multi Scale Mechanics, Faculty of Engineering Technology, University of Twente, P.O. Box 217, 7500 AE Enschede, The Netherlands
[2] Computational BioPhysics, Faculty of Science and Technology, University of Twente, P.O. Box 217, 7500 AE Enschede, The Netherlands
[3] MESA+ Institute for Nanotechnology, University of Twente, P.O. Box 217, 7500 AE Enschede, The Netherlands
[4] Forschungszentrum Jülich, ICS 3, D-52425 Jülich, Germany

The clathrin model

This supplementary material describes the main features of our coarse-grained clathrin model. We refer the interested reader to earlier publications for more details and a motivation of the model.

Shape

The particle is rigid. Each leg consists of a three linear segments, referred to as the proximal (p), distal (d) and terminal domain (td), see Fig 1. The three proximal segments meet at the central hub (h), at a pucker angle $\chi = 101°$ relative to the normal vector $\hat{\mathbf{n}}_h$ along to the three fold symmetry axis of the particle. Normal vectors are also associated with every knee (k); the normal $\hat{\mathbf{n}}_{\alpha,k}$ of the knee of the α^{th} leg lies in the plane formed by the proximal segment of that leg and the particle normal $\hat{\mathbf{n}}_h$. The three angles between a knee-normal and the two leg segments meeting at that knee are chosen to be identical to the three angles between the hub-normal and two proximal segments meeting at the hub. The terminal domain is attached at the ankle (a) at an angle of 114° relative to the adjacent distal segment, and at a dihedral angle of 28° relative to the distal and proximal segments of the same leg. All leg segment are taken to be the same length, $\sigma = 17\,\text{nm}$. Associated with every proximal segment is a polarity vector, defined for the α^{th} leg as

$$\hat{\mathbf{m}}_{\alpha,p} = \frac{(\mathbf{x}_{\alpha,k} - \mathbf{x}_h) \times \hat{\mathbf{n}}_h}{|(\mathbf{x}_{\alpha,k} - \mathbf{x}_h) \times \hat{\mathbf{n}}_h|}, \tag{1}$$

with $\mathbf{x}$ denoting the position of the specific joint indicated in the subscript, see Fig. S1. Polarity vectors to distal segment $\hat{\mathbf{m}}_{\alpha,d}$ are defined likewise, based on the end points of that segment and the normal at the knee.

Potential

The interaction between two triskelia is described by a sum of inter-segmental interactions. These interactions conform with the segmental pairings observed in experimental cage

edges: attractive interactions are introduced between aligned pairs of two anti-parallel proximal segments, of two anti-parallel distal segments, and between any aligned pair of one proximal and one distal segment; here 'anti-parallel' refers to amino acid sequences running in opposite directions. When two segments are properly aligned, their respective ends are close to each other. As an example, consider the proximal segment of the α^{th} leg of particle i interacting with the proximal segment of the β^{th} leg of particle j. The two average distances between the four ends of these segments are

$$r_{j\beta,kh}^{i\alpha,hk} = \frac{1}{2}\left|\mathbf{x}_{i,h} - \mathbf{x}_{j\beta,k}\right| + \frac{1}{2}\left|\mathbf{x}_{i\alpha,k} - \mathbf{x}_{j,h}\right|, \tag{2}$$

$$r_{j\beta,hk}^{i\alpha,hk} = \frac{1}{2}\left|\mathbf{x}_{i,h} - \mathbf{x}_{j,h}\right| + \frac{1}{2}\left|\mathbf{x}_{i\alpha,k} - \mathbf{x}_{j\beta,k}\right|, \tag{3}$$

where the distance on the first line is small if the hub of i is close to the β^{th} knee of j and the α^{th} knee of i is close to the hub of j (*i.e.* aligned and anti-parallel), while the distance on the second line is small if the hub of i is close to the hub of j and the α^{th} knee of i is close to the β^{th} knee of j (*i.e.* aligned and parallel), as illustrated in Fig. S2. The former combination occurs in clathrin cages, hence an attractive interaction is assigned:

$$\phi_{j\beta,kh}^{i\alpha,hk} = -\varepsilon_{kh}^{hk} \cdot f\left(r_{j\beta,kh}^{i\alpha,hk}\right) \cdot g\left(\hat{\mathbf{m}}_{i\alpha,p} \cdot \hat{\mathbf{m}}_{j\beta,p}\right), \tag{4}$$

with the positive parameter ε_{kh}^{hk} denoting the (absolute) maximum inter-segmental binding energy. The distance dependence smoothly decreases from unity for coinciding end points to zero at the cut-off distance r_{cut}, following

$$f(r) = \frac{1}{2}\left[1 - \frac{\tanh[A(r - r_{\text{cut}}/2)]}{\tanh[Ar_{\text{cut}}/2]}\right], \tag{5}$$

where A determines the steepness of the potential, see Fig. S3. The numerical values entering these expressions are provided in Table S1. In addition to a small distance between the end points, we also require alignment of the polarities of the two leg segments, through

$$g(x) = \begin{cases} -x & \text{for} \quad x < 0 \\ 0 & \text{for} \quad x \geq 0. \end{cases} \tag{6}$$

This factor reflects the supposition that interaction sites are not distributed homogeneously over the segmental surface, but are concentrated on the side that faces the three neighbouring segments in a cage edge. As a result, two legs will bind only if the two triskelia involved are oriented similarly, *i.e.* their hub normals point approximately in the same direction. For the current example of two proximal segments, they will bind only if the average hub-knee distance is small and their polarities are pointing in opposite directions. Our earlier simulations indicated that this rotational asymmetry holds the key to the self-assembly of clathrin cages; upon removing the factor g from the potential, triskelia form disordered aggregates rather than cages. All other attractive interactions between binding segment pairs, see the aforementioned list of combinations, are constructed along the same lines.

The introduction of excluded volume interactions between the thin long legs is disadvantageous from a computational point of view: they impose a smaller time step, and the legs have to be non-linear and slightly flexible in order to interweave into a cage edge. We therefore omitted excluded volume interactions. One important consequence of excluded volume interactions should not be ignored, however: excluded volume prevents a leg segment from binding to an edge in a 'slot' already occupied by another leg segment.

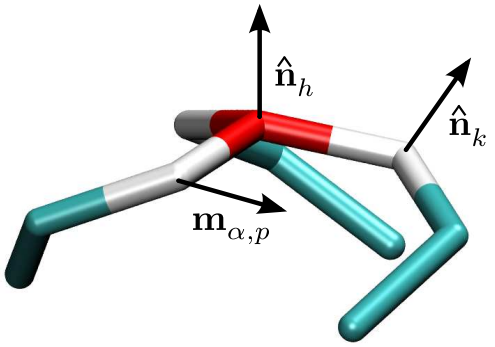

Figure S1: The coarse grained simulation model. The unit vectors $\hat{\mathbf{n}}_h$ and $\hat{\mathbf{m}}_{\alpha,p}$ denote the normal at the hub and the polarity vector of a proximal segment, respectively.

Returning to the two proximal segments of the above example: the distance between the ends of two aligned parallel proximal segments, as calculated in Eq. (3), should not become small. This is achieved by a pair interaction similar to Eq. (4),

$$\phi^{i\alpha,hk}_{j\beta,kh} = -\varepsilon^{hk}_{hk} \cdot f\left(r^{i\alpha,hk}_{j\beta,hk}\right), \tag{7}$$

where the interaction strength parameter ε^{hk}_{hk} has a negative value and the rotational asymmetry has been omitted. A likewise interaction is introduced between two aligned parallel distal segments. The parameters of these repulsive interactions are listed in Table S1.

$i\alpha - j\beta$	ε	A/σ^{-1}	r_{cut}/σ	$g(x)$
attractive				
$hk - kh$	ϵ	4	0.4	$\hat{\mathbf{m}}_p \cdot \hat{\mathbf{m}}_p$
$ka - ak$	ϵ	4	0.4	$\hat{\mathbf{m}}_d \cdot \hat{\mathbf{m}}_d$
$hk - ka$	$\epsilon/2$	4	0.4	$-\hat{\mathbf{m}}_p \cdot \hat{\mathbf{m}}_d$
$hk - ak$	$\epsilon/2$	4	0.4	$\hat{\mathbf{m}}_p \cdot \hat{\mathbf{m}}_d$
repulsive				
$hk - hk$	-10ϵ	0.8	0.8	-1
$ka - ka$	-10ϵ	0.8	0.8	-1

Table S1: Interaction parameters of the six distinct clathrin leg segment pairings. In the first column, the letters refer to the hub (h), knee (k) and ankle (a) of legs α and β of particles i and j, respectively. Note that the order is important: the two proximal-proximal pairings, *i.e.* the first attractive combination and the first repulsive combination, refer to Eqs. (2) and (3), respectively. The value of ϵ is varied from 2 to $10k_BT$ in the construction of the phase diagrams. The elements in the last column represent the arguments x to the polarity function $g(x)$, where the first vector in the dot products refers to a segment of the α leg of particle i and the second vector to a segment of the β leg of particle j, and where $g(-1) = 1$.

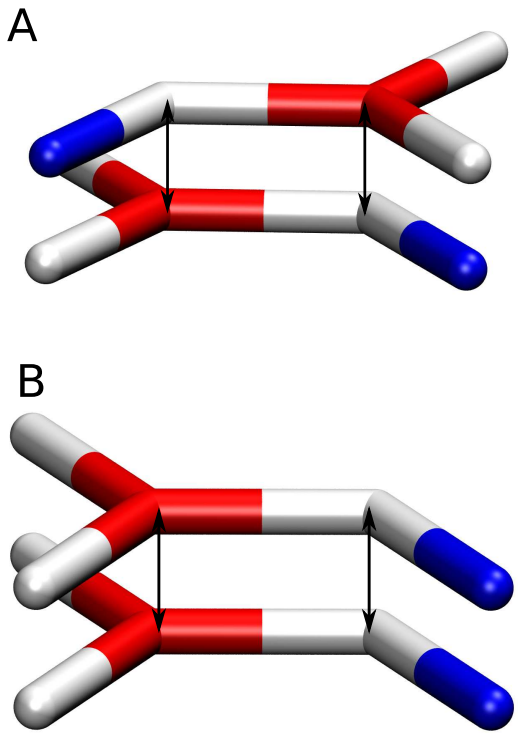

Figure S2: (A) Arrows indicating the two distances entering Eq. (2), to be used for the attractive potential, and (B) arrows indicating the two distances entering Eq. (3), to be used for the repulsive potential.

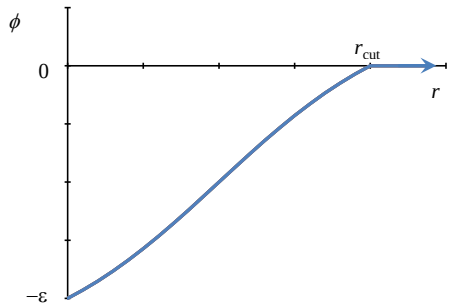

Figure S3: Distance dependence of the segment-segment interaction.

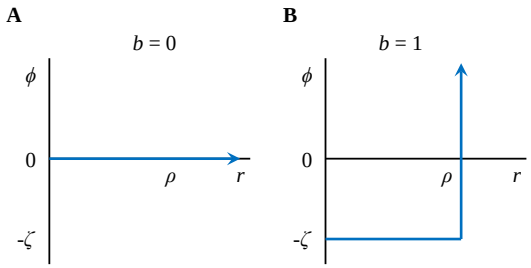

Figure S4: AP-clathrin click potential in the unclicked (A, $b = 0$) and clicked (B, $b = 1$) state.

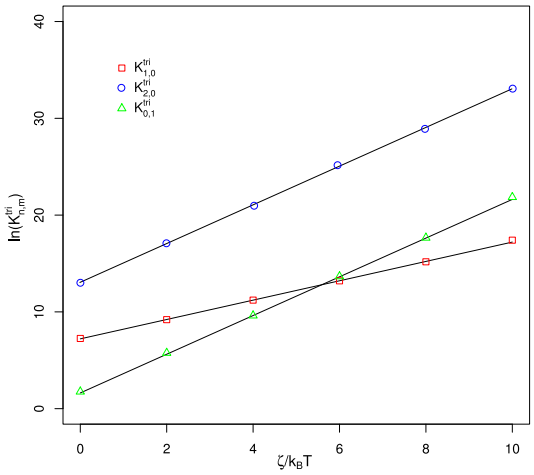

Figure S5: Validation of the Monte Carlo clicking moves by comparing reaction equilibrium constants obtained from simulations (markers) with the theoretical expressions (solid lines) derived in Appendix 1. Shown are the reaction equilibrium constants for triskelia with one single-clicked AP, $K^{\text{tri}}_{1,0}$, with two single-clicked APs, $K^{\text{tri}}_{2,0}$, and with one double-clicked AP, $K^{\text{tri}}_{0,1}$. Simulations are performed using a box of volume $10^6\sigma^3$ populated with 1,000 clathrin and 3,000 APs. To enhance the number of clicks and to facilitate the comparison with theory, the clathrin-clathrin interactions are turned off, $\epsilon = 0$, AP clicks are limited to one leg per triskelion, the AP spring constant is reduced to $k = 1k_BT/\sigma^2$, and the radius of the click interaction is enlarged to $\rho = 0.3\sigma$.

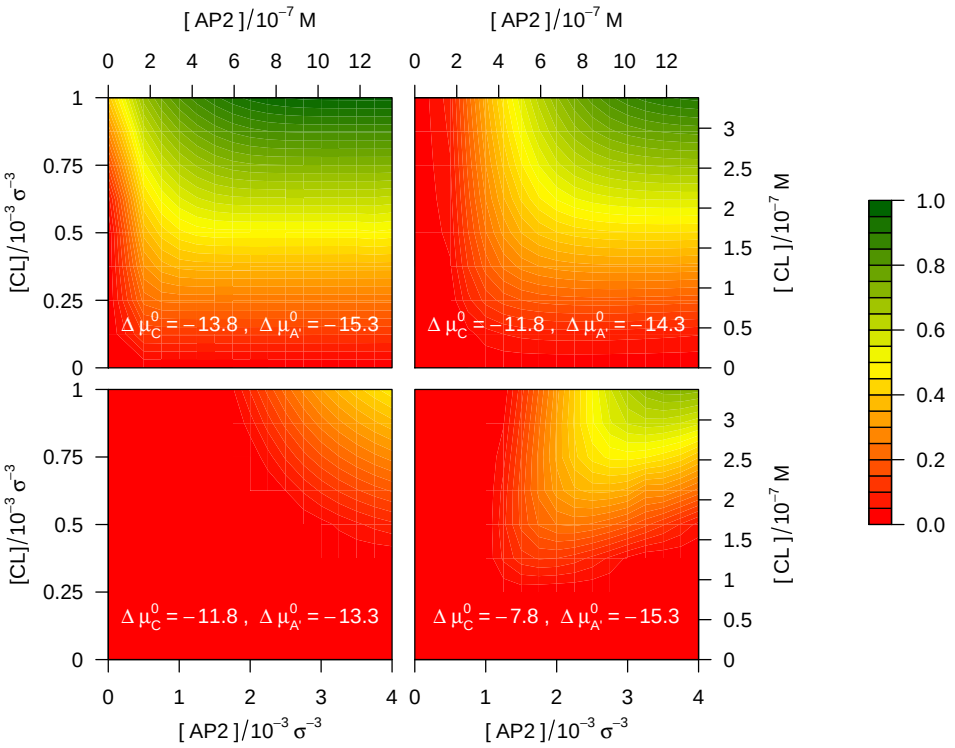

Figure S6: Calculated fraction of triskelia absorbed in cages, for APs clicking to the ends of the TDs and the ankles of triskelia, as a function of the clathrin and AP concentrations, for the standard chemical potential differences indicated on the plots, in units of k_BT. See main text for discussion.